INT. J. ELECTRONICS, 1986, VOL. 60, NO. 2, 229–238

Radiation characteristics of the corner array

H. A. RAGHEB†, A. Z. ELSHERBENI† and M. HAMID†

The paper describes an optimization of Schell's design of the corner array, which is a corner reflector fed by an array of dipoles along the axis, in order to take into account the edge diffraction, mutual coupling between, and off-axis positioning of the radiators, as well as arbitrary corner angles. Numerical examples are presented to illustrate the optimization procedure and significant resulting improvement in the radiation characteristics.

1. Introduction

The analysis of the corner reflector antenna was investigated extensively by Moullin (1945), Kraus (1940), Wait (1954), Neff and Tillman (1954), Willson and Cottony (1960), Ohba (1960), Klopfenstein (1957) and others.

The corner array was originally introduced by Schell (1959) to improve the directivity and gain of the ordinary corner reflector antenna. It should be mentioned that in Schell's analysis the off-axis positioning of the radiators, the mutual coupling between the radiator, and between the radiators and the reflecting sheets as well as the edge diffraction of the reflectors, are ignored. In order to complete the design analysis, these factors are investigated and numerical examples are presented to illustrate the optimization procedure and significant resulting improvement in the radiation characteristics.

2. Analysis and design procedure

A schematic diagram of the general corner array and the coordinate system used is illustrated in Fig. 1. The feed array consists of N infinitesimal dipoles each of length $2H$. The proper choice of position and the excitation currents of the elements may yield higher gain for an optimum array pattern. In the following analysis and proposed design of the corner array, the reflector angle ψ is taken as a submultiple of π and the reflector length is assumed to be infinite. Upon applying the image theory, the far electric field from the corner array is given by

$$E_\theta = \frac{2j\omega\mu H}{4\pi} \frac{\exp(-j\beta r)}{r} \sin\theta\, S(\theta, \phi) \tag{1}$$

where

$$S(\theta, \phi) = \frac{8\pi}{\psi} \sum_{n=1}^{\infty} (-1)^{n\pi/2\psi} \left[\sum_{m=1}^{N} I_m J_{n\pi/\psi}(\beta\rho_m \sin\theta) \times \sin n\pi\left(\frac{\alpha_m}{\psi} + \frac{1}{2}\right)\right] \sin n\pi\left(\frac{\phi}{\psi} + \frac{1}{2}\right) \tag{2}$$

Received 24 June 1985; accepted 11 July 1985.

† Antenna Laboratory, Department of Electrical Engineering University of Manitoba, Winnipeg, Canada R3T 2N2.

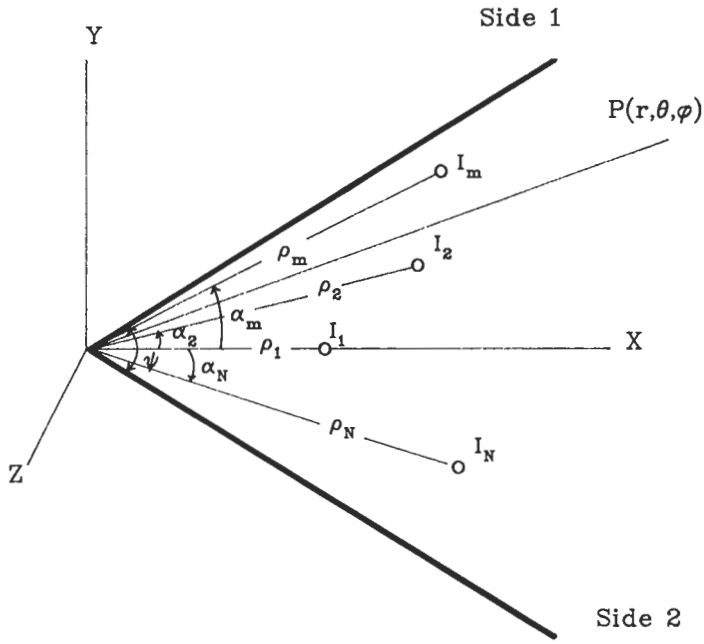

Figure 1. Schematic of corner array.

and ρ_m is the radial distance between the apex and the mth dipole, α_m is the offset angle of the mth dipole, μ is the permeability, ω is the angular frequency, β is the propagation constant $2\pi/\lambda$, λ is the wavelength and $J_n(x)$ is the Bessel function of order n and argument x. It should be mentioned that although (1) is derived from image theory for corner angles equal to submultiples of π, it can be used for any arbitrary corner angle (Klopfenstein, 1957). The only analytical difficulty in generalizing (1) is that S is not equal to zero when ϕ equals $2\pi + \psi/2$ unless ψ is a submultiple of π. However, since ϕ is restricted to the range $-\psi/2 < \phi < \psi/2$ owing to the semi-infinite walls, (1) is valid and general for arbitrary corner angles.

When the feed array elements are located on the bisector of the corner angle, (2) can be written as

$$S(\theta, \phi) = \frac{8\pi}{\psi} \sum_{\substack{n=1 \\ \text{odd}}}^{\infty} (-1)^{nM/2} \left[\sum_{m=1}^{N} I_m J_{nM}(\beta \rho_m \sin \theta) \right] \cos (nM\phi) \tag{3}$$

where $M = \pi/\psi$.

At $\theta = \pi/2$ the far field radiation pattern of a corner array fed by N infinitesimal dipoles located on the bisector of the corner angle is given by

$$S\left(\frac{\pi}{2}, \phi\right) = A_1 \cos (M\phi) + A_2 \cos (3M\phi) + A_3 \cos (5M\phi) + \ldots \tag{4}$$

where

$$A_l = \frac{8\pi}{\psi} (-1)^{(2l-1)M/2} \sum_{m=1}^{N} I_m J_{(2l-1)M}(\beta \rho_m), \qquad l = 1, 2, \ldots \tag{5}$$

The directive gain can also be found by comparing the radiation intensity in the preferred direction, (θ_1, ϕ_1), to the total radiated power as defined by Silver (1947); i.e.

$$D(\theta_1, \phi_1) = \frac{4\pi \sin^2 \theta_1 |S(\theta_1, \phi_1)|^2}{\psi \int_0^{\pi/2} \left| \sum_{\substack{n=1 \\ \text{odd}}}^{x} (-1)^{nM} \left[\sum_{m=1}^{N} I_m J_{nM}(\beta\rho_m \sin \theta) \right]^2 \right| \sin^3 \theta \, d\theta} \tag{6}$$

To start the design procedure, the farthest permissible distance of the dipoles from the apex should be specified in order to truncate the series (4) after a certain number of terms when the higher order Bessel functions approach zero. It is already known (Kraus, 1950) that, for a large distance between the apex and a single feed element, a pattern with more than one main lobe is obtained. Also, numerical computations show that as the spacing between the farthest dipole and the apex is increased further and further, the beamwidth starts to increase and, accordingly, the antenna gain decreases while the pattern will have more than one main beam. For this purpose the maximum permissible distance from the apex (ρ_{max}) in the design procedure is given by the empirical expression

$$\rho_{max} = [180(2N + 1) - 3\psi]/\beta\psi \tag{7}$$

According to this limiting value, the constant A_{N+1} will be approximately equal to zero and the series (4) can be truncated after N terms. The constants $A_1, A_2 \ldots$ and A_N can be evaluated next using the Dolph–Chebyshev procedure by imposing (4) to generate an optimum pattern with minimum beamwidth for a specified main to sidelobe level. Once the value of the constants A_l are evaluated, the excitation currents I_m can be determined from (5) if the element locations ρ_m are specified. In order to determine ρ_m such that the resulting gain is maximum, an optimization process dealing with N variables inherent in the objective function can be done. An optimization routine is used to search for the global maximum of a function of N variables. In our case the gain is taken to be an objective function and the element locations are the variables. The search routine specifies values for the variables within the constraints imposed on it and the gain is then calculated.

The mutual coupling effect considered after determining the optimum element locations for an array of half-wave dipoles. First, the current distribution along each dipole in the feed array is evaluated using an approximate method for solving an appropriate integral equation given by King *et al.* (1968). The resulting current distribution along the mth dipole in the feed array is then given by

$$I_{zm} = jA_m \sin \beta(H - |z|) + B_m(\cos \beta z - \cos \beta H) \tag{8}$$

where A_m and B_m are coefficients which can be evaluated from the geometry of the array and the driving point voltages or currents. This current distribution is used for the calculation of the radiation pattern in which the resultant far field is given by

$$E_\theta = \frac{4j\eta}{\psi} \frac{\exp(j\beta r)}{r} \sum_{\substack{n=1 \\ \text{odd}}}^{x} (-1)^{n\pi/\psi} \left\{ \sum_{m=1}^{N} J_{n\pi/\psi}(\beta\rho_m \sin \theta) \times [jA_m F(\theta, \beta H) + B_m G(\theta, \beta H)] \right\} \cos\left(\frac{n\pi\phi}{\psi}\right) \tag{9}$$

η is the free space impedance, and

$$F(\theta, \beta H) = \frac{2}{\beta} \frac{\cos(\beta H \cos\theta) - \cos(\beta H)}{\sin\theta}$$

$$G(\theta, \beta H) = \frac{2}{\beta} \frac{\sin(\beta H)\cos(\beta H \cos\theta) - \cos(\beta H)\sin(\beta H \cos\theta)}{\sin\theta \cos\theta}$$

Since the mutual coupling is involved in the solution, the resulting radiation pattern is affected and the optimum design parameters calculated without mutual coupling consideration are no longer optimum. In this case a modification in the excitation currents is introduced to evaluate the optimum pattern again.

To evaluate the radiation characteristics of the corner array with finite side walls, two methods are employed.

First we look at the integral equation formulation (IEF), in which the feed array consists of N line sources positioned anywhere between the finite reflector walls. On the surface of the reflector, the total tangential E_z field, which is the sum of the incident and the scattered field, must be equal to zero; i.e.

$$E_z^s + E_z^i = 0$$

where s and i denote the scattered and incident fields, respectively. These fields are given by

$$E_z^s = \frac{\omega\mu}{4} \int_{\text{reflector}} J_z(\rho') H_0^{(2)}(\beta |\bar{r} - \bar{\rho}'|)\, d\rho' \tag{10}$$

$$E_z^i = \sum_{m=1}^{N} \frac{-\omega\mu}{4} I_m H_0^{(2)}(\beta |\bar{r} - \bar{\rho}_m|) \tag{11}$$

where $\bar{\rho}'$ is a vector from the origin to a point on the reflector surface, J_z is the z component of electric surface current density, $H_0^{(2)}$ is the zero-order Hankel function of the second kind, and I_m is the feed current. The resulting integral equation is solved using the moment method to evaluate J_z. Since the far field radiation pattern is the sum of the fields from the current on the reflector surface and the field from the array sources, E_θ becomes

$$\begin{aligned} E_\theta = \sum_{m=1}^{N} \left(\frac{-\mu\omega}{4}\right) I_m \exp\left[j\beta\rho_m \cos(\phi - \alpha_m)\right] \\ + \left(\frac{\omega\mu}{4}\right)\left\{\int_{\text{side 1}} J_z(\rho') \exp\left[j\beta\rho' \cos(\psi/2 - \phi)\right] d\rho' \right. \\ \left. + \int_{\text{side 2}} J_z(\rho') \exp\left[j\beta\rho' \cos(\psi/2 + \phi)\right] d\rho' \right\} \end{aligned} \tag{12}$$

Second, the analysis of the corner reflector with finite width based on the geometrical theory of diffraction (GTD) given by Ohba (1960) is extended here to the corner array. As an example for the 60° corner angle with one feed element (shown in Fig. 2), the entire space is divided into 22 regions by planes which contain the dipole and edge, an image of the dipole and edge, an edge and edge image, or two edges. It should be mentioned that the procedure for subdividing the space for the other sources in the feed array can be drawn in a similar manner and the resulting

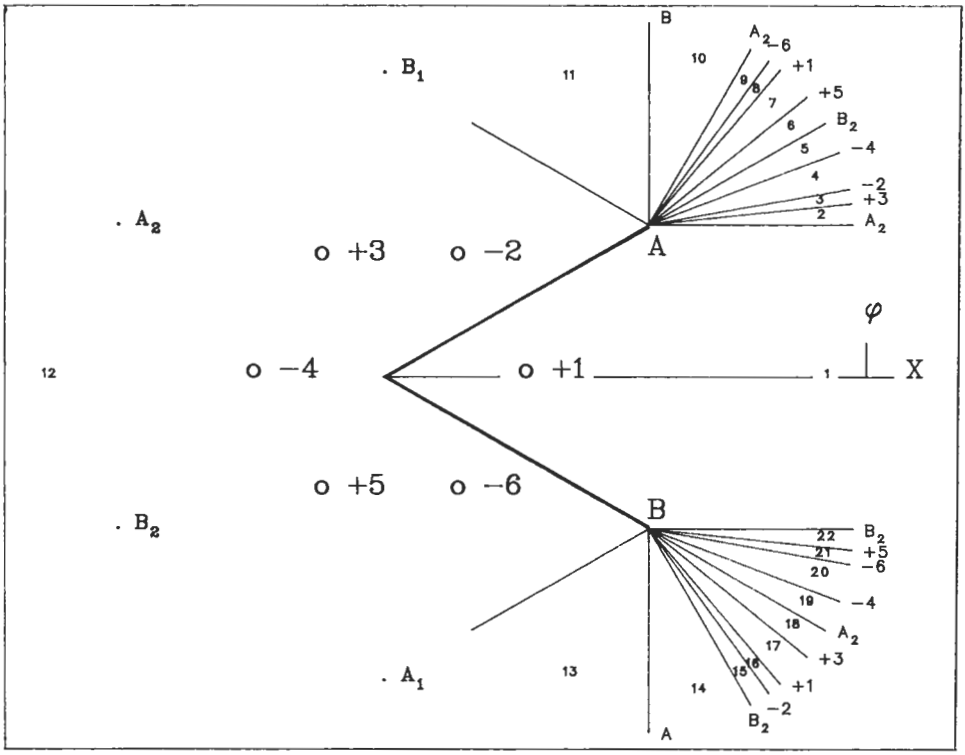

Figure 2. Diagram of images, edge images and the different regions of 60° corner reflector.

regions will be taken into consideration. The total far field in region 1 for all elements of the feed array is given by

$$E_\theta = E_0 \sum_{m=1}^{N} I_m \sum_{n=1}^{6} \exp\{j\beta\rho_m \cos[\phi - (n-1)\pi/3]\} F_1^{(m)}(n) \tag{13}$$

where $E_0 = \exp(j\beta r)/r$, and

$$F_1^{(m)}(n) = 1 - \tfrac{1}{2}[X(T_{nA}^{(m)}) + X(T_{nB}^{(m)}) + X(T_{nA2}^{(m)} + X(T_{nB2}^{(m)})]$$

$$T_{nA} = \beta(R_{nA} - R_n)$$

$$X(T) = [1 - C(T) - S(T)] + j[S(T) - C(T)]$$

and where $C(T)$ and $S(T)$ are Fresnel cosine and sine functions and R_{nA} is the distance between the dipole or the image and the edge plus the distance from the edge to the field point P. T_{nB}, T_{nA2} and T_{nB2} can be evaluated in the same way as T_{nA}. Moreover, the far field in all other regions is evaluated by a similar procedure.

3. Results and discussion

Table 1 illustrates the design parameters corresponding to Schell's and our design for a 60° corner array with three driven elements. Schell's design leads to a gain of 16·9 dB, a beamwidth of 10·3° and a first sidelobe level of −17 dB. For the same case (i.e. on-axis) our search produced a new design which leads to a gain of

Design parameter	Schell design	New design	
		on-axis	off-axis
ρ_1/λ	0·64	0·3	2·35
ρ_2/λ	1·58	1·1	0·315
ρ_3/λ	2·74	2·433	2·35
I_1	0·775	1·0	1·0
I_2	−1·25	−0·336	−0·60
I_3	1·0	0·3	1·0
α_1	0·0	0·0	−15
α_2	0·0	0·0	0·0
α_3	0·0	0·0	15

Table 1. Design parameters of 60° corner array (three driven elements).

19·7 dB, beamwidth of 10·2° and a first sidelobe level of −19·6 dB, as shown in Fig. 3. Figure 4 shows a comparison between the radiation patterns of Schell's design and our new off-axis design. The figure indicates a modest decrease in the beamwidth and the main to sidelobe level by 0·6° and 1·3 dB, respectively.

Table 2 illustrates the design parameters of a 50° corner array fed by three driven elements, where $|I_m|$ and θ_m denote the magnitude and phase of the excitation currents in the mth element, respectively. Figure 5 shows the radiation pattern of the 50° corner array having the design parameters in Table 2. The results obtained for this case indicate that the gain is 19·8 dB while the main to sidelobe level is 20·1 dB and the beamwidth is 8·4°, which are better than all other cases of

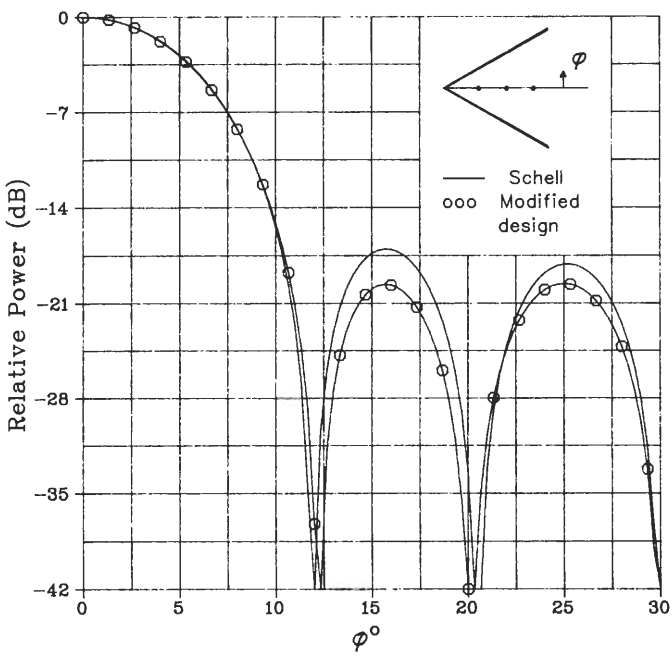

Figure 3. Radiation pattern for on-axis case.

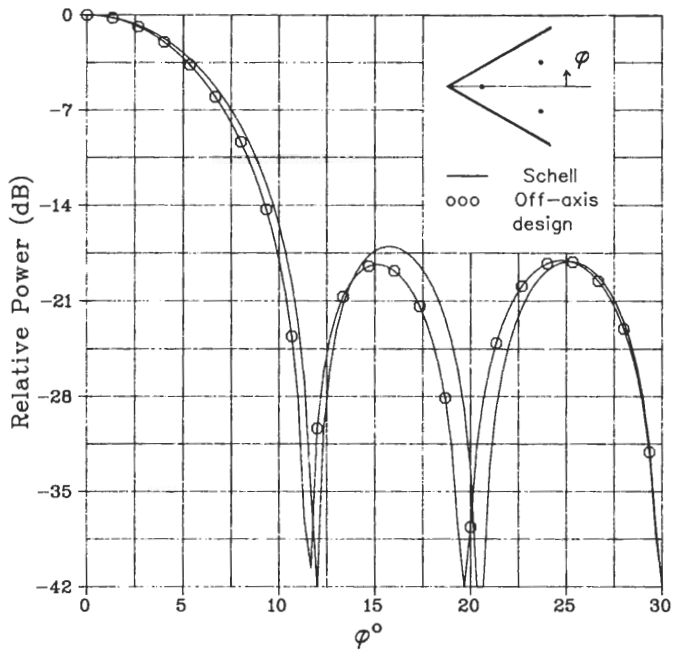

Figure 4. Radiation pattern for off-axis case.

60 corner arrays given before. However, the only disadvantage is that the furthest element of the feed array is at $3{\cdot}1\lambda$ away from the apex, which is a relatively large distance and makes the antenna size larger than that of the 60° case. The 50° corner angle shows that the above analysis and design procedure can be generalized for arbitrary corner angles and illustrates one of the parameters not specifically emphasized by Schell.

By introducing the coupling effect, it is found that the first sidelobe level increases by about 2 dB for some cases. However, by readjusting the excitation currents, the sidelobe level returns to its optimum value as given above. Figure 6 shows the improvement over Schell's design when the mutual coupling effect is taken into account in the feed elements. Also, for the off-axis case, the mutual coupling effects are very small and negligible due to the symmetrical arrangement of the feed array. The above examples are calculated for an infinite wall length to ignore the edge diffraction contribution as well as to confirm that the design given by Schell was not optimum.

	Element 1	Element 2	Element 3
I_m	1·00	0·914	0·775
θ_m	178·6	92·7	−179·4
ρ/λ	1·30	1·90	3·10
α_m	0·00	0·00	0·00

Table 2. Design parameters of 50 corner array (three driven elements).

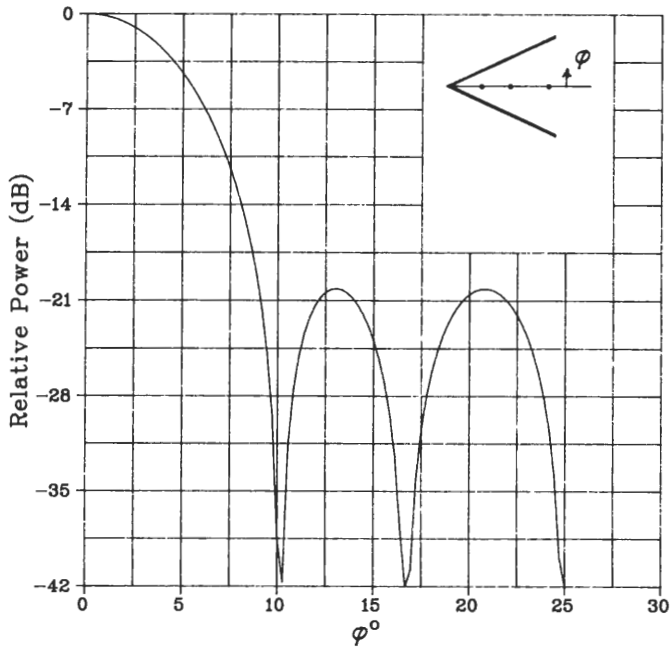

Figure 5. Radiation pattern of 50° corner array.

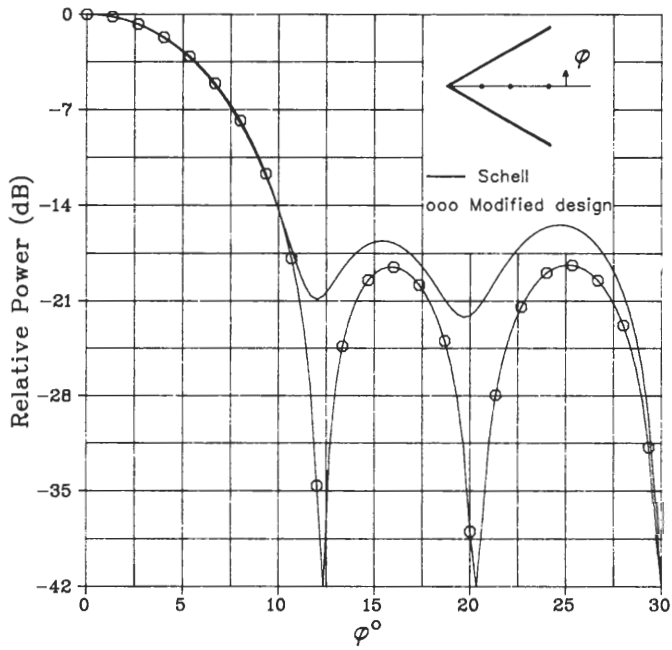

Figure 6. Radiation pattern of 60° corner array with mutual coupling effect.

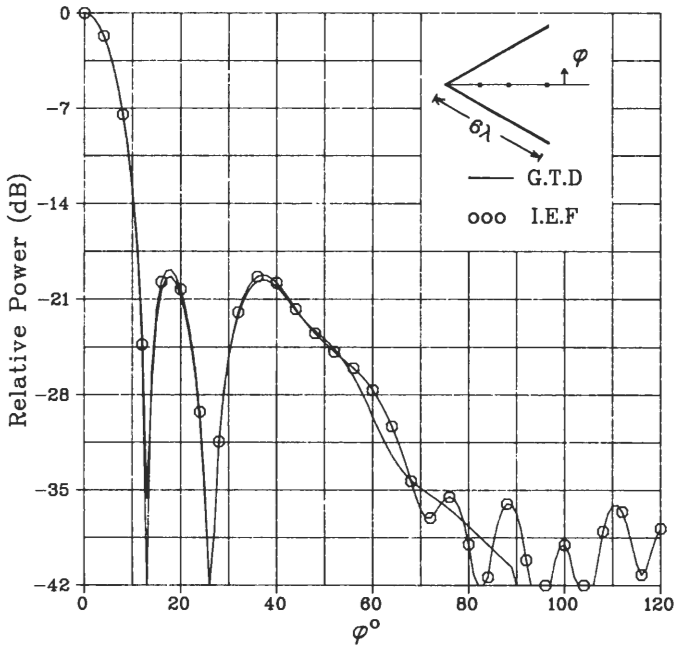

Figure 7. Radiation pattern of finite 60° corner array (on-axis case).

Regarding the edge diffraction effect, Schell's design for a reflector of wall length 6λ yields a sidelobe level of $-17{\cdot}5$ dB, whereas our design of the on-axis case (see Fig. 7) yields $-19{\cdot}3$ dB. The beamwidth in both cases is the same and equals $10{\cdot}5°$. It is found that the sidelobe level is improved by 1·3 dB for a reflector length of 5λ, and by 2 dB for a reflector length of 7λ.

4. Conclusions

This paper has confirmed the possibility of obtaining increased directivity and gain of an ordinary corner reflector antenna by increasing the number of sources within the reflector. The optimum locations of the radiating elements and the application of the Dolph–Chebyshev technique to calculate the optimum pattern and gain have been obtained for N radiators positioned on or off the axis. The corner angle, which was restricted by Schell to an integral fraction of 180°, has also been made arbitrary to allow further extensions to the analysis of the corner array. The practical effect of the element-to-element coupling and edge diffraction have also been investigated. It has been found that the mutual coupling has a significant effect on the main-to-sidelobe level as well as on the gain and beamwidth. This effect is highly dependent on the element-to-element spacing and excitation currents. It is also found that edge diffraction is an important factor in determining the correct sidelobe level. It might be more useful to base the optimum design on the wall current distribution rather than on the far field characteristics. Since the optimum current distribution corresponding to the far field optimum was not specifically calculated, the feasibility of such a procedure would have to be evaluated by further research.

Acknowledgment

The authors wish to acknowledge the financial assistance of the Faculty of Graduate Studies of the University of Manitoba and the Natural Sciences and Engineering Council of Canada which made this research possible.

References

King, R. W., Mack, R. B., and Sandler, S. S., 1968, *Arrays of Cylindrical Dipoles* (Cambridge: Cambridge University Press).

Klopfenstein, R. W., 1957, Corner reflector antennas with arbitrary dipole orientation. *I.R.E. Trans. Antennas Propag.*, **5**, 297.

Kraus, J. D., 1940, The corner reflector antenna. *Proc. Inst. Radio Engrs*, **28**, 513.

Moullin, E. B., 1945, Theory and performance of corner reflector for aerials. *J. Instn elect. Engrs*, Pt. III, **92**, 58.

Neff, H. P., and Tillman, J. J., 1959, The design of the corner reflector antenna. *Commun. Electron.*, **43**, 293.

Ohba, Y., 1960, On the radiation pattern of a corner reflector finite in width. *I.E.E.E. Trans. Antennas Propag.*, **11**, 127.

Schell, A. C., 1959, *The Corner Array*, Air Force Cambridge Research Center, TR-59-105, Bedford, Mass., U.S.A.

Silver, S., 1947, *Microwave Antenna Theory and Design* (New York: McGraw-Hill).

Wait, J. R., 1954, On the theory of an antenna with an infinite corner reflector. *Can. J. Phys.*, **32**, 365.

Willson, A. C., and Cottony, H. V., 1960, Radiation pattern of finite size corner reflector antenna. *I.R.E. Trans. Antennas Propag.*, **8**, 144.